Rasmussen, B., et al., 2021, Apatite nanoparticles in 3.46–2.46 Ga iron formations: Evidence for phosphorus-rich hydrothermal plumes on early Earth: Geology, v. 49, https://doi.org/10.1130/G48374.1

Supplemental Material for:

Apatite nanoparticles in 3.46–2.46 Ga iron formations: Evidence for phosphorus-rich hydrothermal plumes on early Earth

Birger Rasmussen, Janet R. Muhling, Alexandra Suvorova, and Woodward W. Fischer

METHODS

Focused ion beam

Lamellae for transmission electron microscopy (TEM) analyses were cut from polished thin sections of laminated cherts enclosing iron-silicate nanoparticles in polished thin sections. Focussed ion beam (FIB) techniques were used to prepare ~100 nm thick TEM lamellae using an *FEI Helios NanoLab G3 CX DualBeam* instrument located at the Centre for Microscopy, Characterisation and Analysis, The University of Western Australia. The areas selected for TEM analysis were first coated with a strip of Pt 2 μm thick to protect the surface, then trenches 7 μm deep were milled on either side of the strip using a Ga ion beam with 30 kV voltage and 9.3 nA current. The lamellae were then cut away from the samples and welded to Cu TEM grids. The lamellae were thinned with the Ga ion beam at 30 kV and 0.79 nA and 0.23 nA, before cleaning at 5 kV and 41 pA, and polishing at 2 kV and 23 pA.

Transmission electron microscopy

TEM data were obtained at 200 kV using an *FEI Titan G2 80–200 TEM/STEM* with *ChemiSTEM* technology located at CMCA, UWA. Bright-field TEM, High-resolution TEM (HRTEM) and high-angle annular dark-field (HAADF) STEM images were collected and processed using TIA (TEM Imaging and Analysis) software from FEI and Digital Micrograph from Gatan Incorporated. Qualitative EDS spectra and hypermaps were collected using an FEI Super-X EDS detector and processed using Bruker Esprit software.

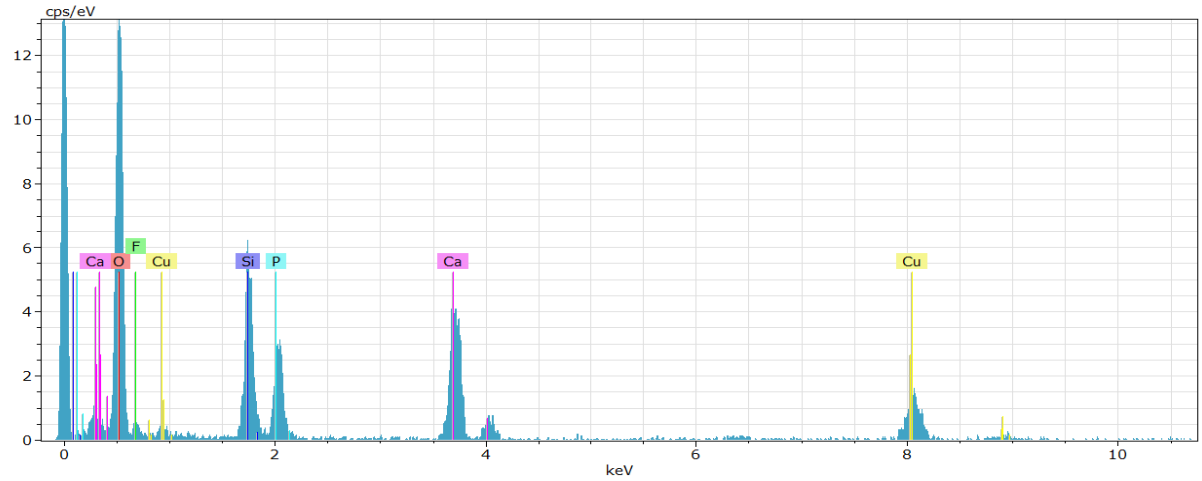

Figure DR1. TEM/EDS spectrum from apatite particle shown in Figure DR2A. Peaks for O, F, P and Ca result from apatite. The peak for Si is from surrounding chert, while the peak for Cu is from the TEM grid. There is no peak for C in the spectrum, suggesting that the grain is fluorapatite.

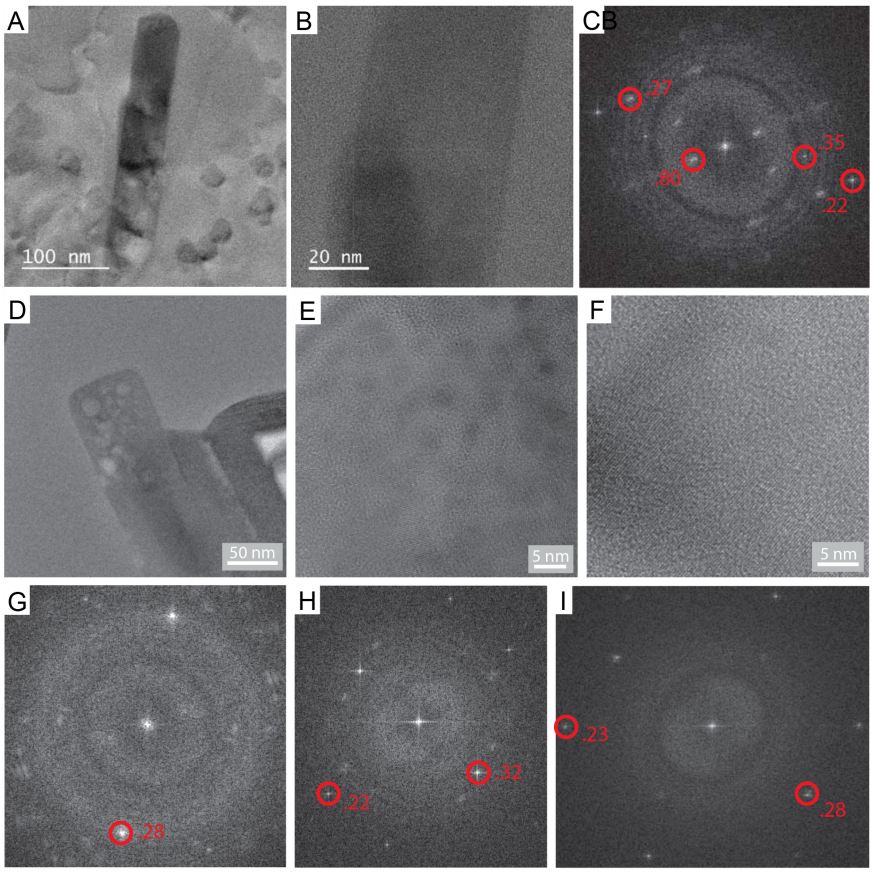

Figure DR2. TEM images of apatite from the Nauga Formation, South Africa. **A**. Bright field image of apatite crystal in quartz. **B**. High-resolution TEM image of grain shown in panel A. **C**. Diffractogram (Fast Fourier Transform: FFT) of part of crystal shown in panel B. Reflections at ca. 0.80 nm, 0.35 nm, 0.27-0.28 nm and 0.21 nm are apparent. **D**. Bright field image of another apatite crystal from the same TEM lamella. **E**. HRTEM image of part of the crystal shown in D showing lattice fringes in several orientations. **F**. Higher magnification image of part of the crystal shown in panel E with only one dominant lattice fringe orientation. **G-I**. Diffractograms from different parts of the crystal shown in panels D-F with reflections at ca. 0.32 nm, 0.28 nm and 0.23 nm. Sample 100315-79B.

Table DR1. Sample identification and summary of nanoparticle phases

Sample ID	Age (Ga)	Formation	Nanoparticles	Phosphate
Silvergrass, 331.5 m	2.46	Joffre Mbr, Brockman Iron Fm, Hamersley Group	Greenalite*	Apatite
Silvergrass, AGC985D	2.48	Dales Gorge Mbr, Brockman Iron Fm, Hamersley Group	Greenalite*	Apatite
Mitchell 2, 418 m	2.5	Colonial Chert Mbr, Mt McRae Shale, Hamersley Group	Greenalite	Apatite
DDH44, 523.75 m	2.5	Colonial Chert Mbr, Mt McRae Shale, Hamersley Group	Greenalite	Apatite
ABDP-9, 221.76-.84 m	2.55	Mt Sylvia Fm, Hamersley Group	Greenalite	Apatite
ABDP-9, 288.23-.36 m	2.56	Bee Gorge Mbr, Wittenoom Fm, Hamersley Group	Greenalite	Apatite
100315-72A	2.58	Nauga Formation, Transvaal Supergroup	Greenalite	Apatite
100315-79B	2.58	Nauga Formation, Transvaal Supergroup	Greenalite	Apatite
95WGD2-6	2.7	Wilgie Mia Formation, Weld Range greenstone belt	Greenalite	Apatite
BPQ-3	3.2	Lower Moodies Group, Barberton Greenstone Belt	Greenalite	Apatite
ABDP-1, 130.60-.70 m	3.46	Marble Bar Chert Mbr, Duffer Fm, Warrawoona Group	Greenalite	Apatite

* Iron-silicate nanoparticles also include stilpnomelane.

Table DR2. TEM diffraction data for apatite (units in nanometers)

Observed	FluorApt					HydApt					CrbApt				
	INTENSITY	D-SPACING	H	K	L	INTENSITY	D-SPACING	H	K	L	INTENSITY	D-SPACING	H	K	L
0.80	9.88	0.81383	1	0	0	13.71	0.8155	1	0	0	2.12	0.8072	1	0	0
	5.36	0.40691	2	0	0	5.75	0.40775	2	0	0	25.5	0.4036	2	0	0
	6.53	0.38798	1	1	1	5.75	0.38846	1	1	1	24.14	0.38611	1	1	1
0.35	37.39	0.34391	0	0	2	34.92	0.34372	0	0	2	16.1	0.34474	0	0	2
0.32	12	0.31679	1	0	2	7.74	0.31674	1	0	2	2.21	0.31703	1	0	2
	14.05	0.3076	1	2	0	14.32	0.30823	1	2	0	3.12	0.30509	1	2	0
											35.51	0.30509	2	1	0
0.28	69.57	0.2808	1	2	1	69.47	0.28125	1	2	1	29.95	0.279	1	2	1
	30.43	0.2808	2	1	1	30.53	0.28125	2	1	1	70.05	0.279	2	1	1
	40.17	0.27752	1	1	2	48.88	0.27762	1	1	2	15.53	0.27715	1	1	2
0.27	57.76	0.27128	3	0	0	61.78	0.27183	3	0	0	64.56	0.26907	3	0	0
	25.65	0.26266	2	0	2	21.89	0.26281	2	0	2	5.3	0.22847	2	1	2
0.22	16.68	0.22572	3	1	0	4.33	0.22618	1	3	0	4.8	0.21211	3	0	2
											24.02	0.20612	1	1	3
											1.14	0.2018	4	0	0

Reflections observed in TEM diffractograms compared with data for fluorapatite, hydroxyl-apatite and carbonate-apatite.

Table DR3. Iron, silica and phosphorus data for Fe oxide-bearing hydrothermal sediments and banded iron formations.

Formation/Sample ID	Age (Ga)	P_2O_5	SiO_2	Fe_2O_3	FeO	Fe_T	Ref.*
East Pacific Rise, Leg 92, site 598							
1-2, 39	0-0.01	0.15				5.01	1
1-2, 49	0-0.01	0.17				6.3	1
1-2, 59	0-0.01	0.26				9.42	1
1-2, 69	0-0.01	0.38				13.22	1
1-2, 102	0-0.01	0.46				14.31	1
1-2, 109	0-0.01	0.42				13.36	1
1-2, 119	0-0.01	0.34				13.3	1
1-2, 129	0-0.01	0.26				10.59	1
1-2, 139	0-0.01	0.17				6.98	1
1-2, 149	0-0.01	0.12				4.83	1
1-3, 9	0-0.01	0.08				3.59	1
1-3, 19	0-0.01	0.08				3.42	1
1-3, 29	0-0.01	0.09				3.76	1
1-3, 39	0-0.01	0.12				5.13	1
1-3, 49	0-0.01	0.18				7.78	1
1-3, 59	0-0.01	0.17				7.86	1
1-3, 69	0-0.01	0.18				8.68	1
1-3,79	0-0.01	0.12				5.98	1
1-3, 89	0-0.01	0.1				4.58	1
1-3, 119	0-0.01	0.12				3.88	1
1-4, 29	0-0.01	0.12				4.59	1
1-4, 39	0-0.01	0.26				8.68	1
1-4,49	0-0.01	0.35				11.06	1
1-4, 59	0-0.01	0.22				7.73	1
1-4, 69	0-0.01	0.1				4.03	1
1-4, 89	0-0.01	0.05				2.27	1
1-4,99	0-0.01	0.06				2.39	1
1-4, 109	0-0.01	0.05				2.18	1
1-4, 119	0-0.01	0.05				2.01	1
1-4, 129	0-0.01	0.08				3.39	1
1-4, 139	0-0.01	0.1				4.56	1
1-4, 149	0-0.01	0.11				4.55	1
Brockman Iron Fm, Hamersley Group, Pilbara Craton, Western Australia							
Dales Gorge Mbr Table 11-1	2.5-2.45	0.25	46.86	24.68	17.19	41.87	2
Dales Gorge Mbr Table 11-2	2.5-2.45	0.22	47.57	27.01	14.47	41.48	2
Dales Gorge Mbr Table 11-3	2.5-2.45	0.19	47.85	25.96	15.15	41.11	2
Dales Gorge Mbr Table 11-4	2.5-2.45	0.24	44.86	29.25	15.58	44.83	2
Dales Gorge Mbr Table 11-5	2.5-2.45		51.44	20.12	14.41	34.53	2
Dales Gorge Mbr Table 11-6	2.5-2.45	0.47	58.05	19.85	12.79	32.64	2
Dales Gorge Mbr Table 11-8	2.5-2.45	0.36	29.6	2.71	36.38	39.09	2

Joffre Mbr Table 11-9	2.5-2.45	0.02	51.63	16.87	17.68	34.55	2
Joffre Mbr Table 11-10	2.5-2.45	0.23	40.61	21.45	17.51	38.96	2
Dales Gorge Mbr Table 11-13	2.5-2.45	0.13	51.54	41.62	6.05	47.67	2
Dales Gorge Mbr Table 12-1	2.5-2.45	0.01	74.71	0.46	8.99	9.45	2
Dales Gorge Mbr Table 12-2	2.5-2.45	0.05	48.41	14.86	19	33.86	2
Dales Gorge Mbr Table 12-3	2.5-2.45	0.45	66.08	1.6	8.68	10.28	2
Dales Gorge Mbr Table 12-4	2.5-2.45	0.09	35.74	35.43	19.71	55.14	2
Dales Gorge Mbr Table 12-5	2.5-2.45	0.22	43.39	6.76	23.32	30.08	2
Dales Gorge Mbr Table 12-6	2.5-2.45	0.12	45.15	7.23	21.92	29.15	2
Dales Gorge Mbr Table 12-7	2.5-2.45	0.16	43.17	7.06	23.99	31.05	2
Dales Gorge Mbr Table 12-8	2.5-2.45	0.08	30.03	4.86	30.01	34.87	2
Dales Gorge Mbr Table 12-9	2.5-2.45	0.1	45.26	8.24	21.6	29.84	2
Dales Gorge Mbr Table 12-10	2.5-2.45	0.28	24.76	5.69	32.93	38.62	2
Dales Gorge Mbr Table 12-11	2.5-2.45	0.31	32.49	4.92	29.44	34.36	2
Dales Gorge Mbr Table 12-12	2.5-2.45	0.42	37.87	5.2	23.36	28.56	2
Dales Gorge Mbr Table 12-13	2.5-2.45	0.48	28.75	9.89	27.87	37.76	2
Dales Gorge Mbr Table 12-14	2.5-2.45	0.48	30.19	13.2	25.87	39.07	2
Dales Gorge Mbr Table 12-15	2.5-2.45	0.66	34.2	8.58	24.55	33.13	2
Dales Gorge Mbr Table 12-16	2.5-2.45	0.14	86.08	0.29	4.25	4.54	2
Dales Gorge Mbr Table 12-17	2.5-2.45	0.12	92.98	0.2	2.12	2.32	2
Dales Gorge Mbr Table 12-18	2.5-2.45	0.46	80.69	0.63	6.37	7	2
Dales Gorge Mbr Table 12-19	2.5-2.45	0.09	53.26	35.56	8.14	43.7	2
Kuruman Iron Formation, Kaapvaal Craton, South Africa							
AD5, 121.3 m; Table 3-1	2.5-2.45	0.06	41.7	1.97	25.69	27.66	3
AD5, 158.4 m; Table 3-2	2.5-2.45	0.05	40.37	1.01	26.21	27.22	3
AD5, 159.3 m; Table 3-3	2.5-2.45	0.03	40.91	1.58	20.71	22.29	3
AD5, 161.9 m; Table 3-4	2.5-2.45	0.1	16.16	1.79	32.79	34.58	3
AD5, 161.95 m; Table 3-5	2.5-2.45	0.08	46.23	3	24.88	27.88	3
AD5, 163.2 m; Table 3-6	2.5-2.45	0.03	41.96	1.08	16.21	17.29	3
AD5, 167.8 m; Table 3-7	2.5-2.45	0.11	32.28	1.18	23.9	25.08	3
AD5, 168.7 m; Table 3-8	2.5-2.45	0.1	18.52		27.19	27.19	3
DI1, 213.8 m; Table 3-9	2.5-2.45	0.08	44.4	0.67	22.12	22.79	3
DI1, 223.8 m; Table 3-10	2.5-2.45	0.01	46.4	1	18.34	19.34	3
DI1, 236.7 m; Table 3-11	2.5-2.45	0.05	57.75	2.94	18.66	21.6	3
DI1, 237.0 m; Table 3-12	2.5-2.45	0.03	11.9	1.56	37.58	39.14	3
WB98, 814.3 m; Table 3-13	2.5-2.45	0.03	44	0.56	26.36	26.92	3
WB98, 816.9 m; Table 3-14	2.5-2.45	0.05	53.8	0.59	20.73	21.32	3
WB98, 866.0 m; Table 3-15	2.5-2.45	0.09	37.9	1.3	25.21	26.51	3
WB98, 882.0 m; Table 3-16	2.5-2.45	0.08	65.5	0.58	15.26	15.84	3
DI1, 221.5 m; Table 3-17	2.5-2.45	0.08	31.62		26.15	26.15	3
WB98, 896.1 m; Table 3-18	2.5-2.45	0.01	65.85	0.13	13.09	13.22	3
DI1, 245.2 m; Table 3-19	2.5-2.45	0.01	69.92		7.98	7.98	3
AD5, 92.5 m; Table 4-1	2.5-2.45	0.08	56.38	15.38	19.47	34.85	3
AD5, 94.4 m; Table 4-2	2.5-2.45	0.1	40	30.93	20.8	51.73	3
AD5, 124.8 m; Table 4-3	2.5-2.45	0.09	42.04	24.96	20.71	45.67	3

DI1, 226.1 m; Table 4-4	2.5-2.45	0.12	49.46	24.83	8.93	33.76	3
DI1, 238.8 m; Table 4-5	2.5-2.45	0.34	51.43	24.3	8.77	33.07	3
AD5, 136.5 m; Table 4-6	2.5-2.45	0.11	44.31	28.52	16.13	44.65	3
AD5, 149.8 m; Table 4-7	2.5-2.45	0.06	37	14.48	21.85	36.33	3
AD5, 152.1 m; Table 4-8	2.5-2.45	0.06	51.57	17.86	17.09	34.95	3
WB98, 791.2 m; Table 4-9	2.5-2.45	0.08	45.17	24.17	21.33	45.5	3
WB98, 791.4 m; Table 4-10	2.5-2.45	0.04	47.3	21.8	20.56	42.36	3
156.85 m, Table III-10	2.5-2.45	0.03	21.3	25.06	23.24	48.3	4
158.3 m, Table III-11	2.5-2.45	0.03	50.7	11.13	13.06	24.19	4
158.35 m, Table III-12	2.5-2.45	0.01	66.51	7.98	9.62	17.6	4
158.8 m, Table III-13	2.5-2.45	0.02	52.1	5.04	12.65	17.69	4
160.97 m, Table III-14	2.5-2.45	0.05	48.22	10.89	19.36	30.25	4
162.34 m, Table III-15	2.5-2.45	0.001	44.35	16.42	20.87	37.29	4
166.1 m, Table III-16	2.5-2.45	0.04	52.9	15.08	12.55	27.63	4
168.78 m, Table III-17	2.5-2.45	0.02	44.3	24.53	15.24	39.77	4
169.24 m, Table III-18	2.5-2.45	0.09	52.2	18.65	13.14	31.79	4
170.25 m, Table III-19	2.5-2.45	0.001	41.23	29.4	17.91	47.31	4
172.75 m, Table III-20	2.5-2.45	0.008	37.3	17.8	21.74	39.54	4
173.16 m, Table III-21	2.5-2.45	0.009	49.94	21.21	16.33	37.54	4
173.20 m, Table III-22	2.5-2.45	0.003	53.44	23.3	14.39	37.69	4
175.94 m, Table III-23	2.5-2.45	0.011	47.92	21.31	17.68	38.99	4
176.5 m, Table III-24	2.5-2.45	0.008	69.22	7.28	13.26	20.54	4
178.4 m, Table III-25	2.5-2.45	0.026	53.01	0.8	14	14.8	4
178.95 m, Table III-26	2.5-2.45	0.015	57	9.27	11.72	20.99	4
178.99 m, Table III-27	2.5-2.45	0.04	24.1	16.48	19.02	35.5	4
180.7 m, Table III-28	2.5-2.45	0.003	45.4	15.45	18.34	33.79	4
187.2 m, Table III-29	2.5-2.45	0.11	23.76	7.25	36.94	44.19	4
187.25 m, Table III-30	2.5-2.45	0.001	82.92	6.04	8.08	14.12	4
187.44 m, Table III-31	2.5-2.45	0.05	42.48	9.02	19.35	28.37	4
189.07 m, Table III-32	2.5-2.45	0.14	52.43	4.92	21.09	26.01	4
189.6 m, Table III-33	2.5-2.45	0.04	37.59	8.04	28.46	36.5	4
193.87 m, Table III-34	2.5-2.45	0.01	55.66	4.06	29.62	33.68	4
Griquatown Iron Formation, Kaapvaal Craton, South Africa							
137.31 m, Table III-1	2.45	0.01	36.79	20.62	18.66	39.28	4
140.8 m, Table III-2	2.45	0.04	37.98	31.38	20.18	51.56	4
142.83 m, Table III-3	2.45	0.06	49.42	17.28	18.17	35.45	4
150.12 m, Table III-4	2.45	0.16	47.3	11.7	10.48	22.18	4
150.25 m, Table III-5	2.45	0.15	48.11	16.87	19.32	36.19	4
152.03 m, Table III-6	2.45	0.04	52.9	13.79	15.65	29.44	4
153.23 m, Table III-7	2.45	0.03	51	13.26	20.78	34.04	4
154.1 m, Table III-8	2.45	0.26	51.8	17.14	16.15	33.29	4
155.7 m, Table III-9	2.45	0.02	53.9	17.42	16.22	33.64	4

*Ref. 1 (Lyle, 1986); 2 (Trendall and Blockley, 1970); 3 (Klein and Beukes, 1989); 4 (Beukes and Klein, 1990).

REFERENCES CITED

Beukes, N.J., and Klein, C., 1990, Geochemistry and sedimentology of a facies transition from microbanded to granular iron-formation in the early Proterozoic Transvaal Supergroup, South Africa: Precambrian Research, v. 47, p. 99–139.

Klein, C., and Beukes, N.J., 1989, Geochemistry and sedimentology of a facies transition from limestone to iron-formation deposition in the Early Proterozoic Transvaal Supergroup, South Africa: Economic Geology, v. 84, p. 1733–1774.

Lyle, M.W., 1986, Major element composition of Leg 92 sediments: Initial Reports of the Deep Sea Drilling Project, v. 92, p. 355-370.

Trendall, A.F., and Blockley, J.G., 1970, The iron-formations of the Precambrian Hamersley Group, Western Australia: Geological Survey of Western Australia Bulletin, v. 119, 366 pp.